

Synthesis, Structure, and Bonding of Sc_6MTe_2 ($\text{M} = \text{Ag}, \text{Cu}, \text{Cd}$): Heterometal-Induced Polymerization of Metal Chains in Sc_2Te

Ling Chen and John D. Corbett*

Department of Chemistry, Iowa State University, Ames, Iowa 50011

Received December 6, 2001

Three new compounds, Sc_6AgTe_2 , $\text{Sc}_6\text{Cu}_{0.80(2)}\text{Te}_{2.20(2)}$, and Sc_6CdTe_2 , were prepared by high-temperature solid state techniques, and the structures were determined by single-crystal X-ray diffraction to be orthorhombic, $Pnma$ (No. 62, $Z = 4$) with $a = 20.094(9)$ Å, $19.853(5)$ Å, $20.08(1)$ Å, $b = 3.913(1)$ Å, $3.914(1)$ Å, $3.915(2)$ Å, and $c = 10.688(2)$ Å, $10.644(2)$ Å, $10.679(5)$ Å, respectively, at 23 °C. The compounds are isotypic with Sc_6PdTe_2 and represent the first ternary metal-rich rare-earth-metal chalcogenides containing group 11 or group 12 elements. The structure can be viewed as heterometal sheets lying parallel to the b – c planes that are separated by isolated tellurium atoms. These sheets can also be viewed as a polymerization of two different types of metal chains in Sc_2Te (blades and zigzag chains) by heterometal (M) replacements of some intervening tellurium atoms. Extended Hückel band calculations reveal that the interior atoms in the metal network achieve negative formal Mulliken charges while Sc atoms on the exterior that have tellurium neighbors have positive values. The heterometal–metal bonding enhances the overlap populations of zigzag chains and blades relative to those in Sc_2Te . The calculation results also indicate that these compounds are metallic, as usual.

Introduction

The nature of stable metal frameworks has been investigated since early works of Zintl, Pauling, and others.¹ Metal-rich chalcogenide phases have attracted attention both because of their rich chemistry that gives insight into the relationships between various metal–metal bonding features² and because of their potential for displaying interesting properties.³ Since Brewer and Wengert first noted the remarkable strengths of polar intermetallic bonding in the 1970s,⁴ heterometal-rich chalcogenides of group 4 and 5 early transition metals have provided a great variety of new chemistry. These studies have recently been successfully extended to group 3 rare-earth elements (R). The divergence in crystal chemistry of group 3 vs 4, 5 is that the smaller number of metal-based electrons in the first appears to force a weakening and a reduction in metal–metal framework dimensionality, for example, in Sc_8Te_3 ⁵ vs Ti_8Se_3 ⁶ and

Sc_2Te^7 vs Zr_2Te .⁸ Furthermore, incorporation of late transition metals has long been known to stabilize both metal-rich halides⁹ and chalcogenides.¹⁰

Many of the recently reported electron-poorer transition-metal-rich chalcogenides have a common structural motif, tricapped trigonal prisms (TTP) of the transition metal centered by a late transition metal. Using TTPs as fundamental building blocks, different structures can be constructed via different condensation schemes, e.g., R_6MTe_2 ($\text{R} = \text{Sc}$,¹¹ Dy ;¹² $\text{M} = \text{Mn}, \text{Fe}, \text{Co}, \text{Ni}$: Fe_2P -type) and $\text{Er}_7\text{Ni}_2\text{Te}_2$.¹³ Some others belong to the Gd_3MnI_3 -type family in which the transition metal occurs in infinite, puckered chains of six-rings as the fundamental building units that sandwich late transition metals, e.g., $\text{Y}_3\text{M}_2\text{Te}_2$ ($\text{M} = \text{Fe}, \text{Co}$,

* Author to whom correspondence should be addressed. E-mail: jdc@ameslab.gov.

- (1) (a) Zintl, E. *Angew. Chem.* **1939**, *52*, 1. (b) Pauling, L. *Phys. Rev.* **1938**, *54*, 899. (c) Pearson, W. B. *The Crystal Chemistry and Physics of Metals and Alloys*; Wiley-Interscience: New York, 1972.
- (2) Whangbo, M. H.; Canadell, E.; Foury, P. *Science* **1991**, *252*, 96.
- (3) *Handbook of Crystal Structures and Magnetic Properties of Rare Earth Intermetallics*; Szytula, A., Leciejewicz, J., Eds.; CRC Press: Boca Raton, FL, 1994.
- (4) Brewer, L.; Wengert, P. R. *Metallurg. Trans.* **1973**, *4*, 2674.

- (5) Maggard, P. A.; Corbett, J. D. *Inorg. Chem.* **1998**, *37*, 814.
- (6) Weirich, T. E.; Pöttgen, R.; Simon, A. Z. *Kristallogr.* **1996**, *211*, 927.
- (7) Maggard, P. A.; Corbett, J. D. *Angew. Chem., Int. Ed. Engl.* **1997**, *36*, 1974.
- (8) Örlýgsson, G.; Harbrecht, B. *Inorg. Chem.* **1999**, *38*, 3377.
- (9) Corbett, J. D. *J. Alloys Compd.* **1995**, *229*, 10.
- (10) Harbrecht, B.; Franzen, H. F. *J. Less-Common Met.* **1986**, *124*, 125. (b) Harbrecht, B. *J. Less-Common Met.* **1988**, *182*, 118. (c) Kleinke, H.; Franzen, H. F. *Inorg. Chem.* **1996**, *35*, 5272. (d) Kleinke, H.; Franzen, H. F. *J. Alloys Compd.* **1997**, *225*, 110.
- (11) Maggard, P. A.; Corbett, J. D. *Inorg. Chem.* **2000**, *39*, 4143.
- (12) Bestaoui, N.; Herle, P. S.; Corbett, J. D. *J. Solid State Chem.* **2000**, *155*, 9.
- (13) Fanqin M.; Hughbanks, T. *Inorg. Chem.* **2001**, *40*, 2482.

Ni)¹⁴ and $Sc_5Ni_2Te_2$.¹⁵ So far, only one ternary compound has been reported to crystallize with the unusual orthorhombic structure of Sc_6PdTe_2 ¹⁴ in which the remarkable bonding of Pd between the two types of metal chains in Sc_2Te_7 produces new heterometal rumpled sheets. Here, we report the synthesis and structures of three new compounds that occur in the same orthorhombic family and represent the first metal-rich ternary chalcogenides that contain group 11 elements Cu, Ag or the group 12 element Cd. The electronic structures of all three Sc_6MTe_2 compounds (M = Ag, Cu, Pd) are also presented and discussed.

Experimental Section

Syntheses. All materials were handled in a He-filled glovebox. The synthesis of Sc_6AgTe_2 began with the preparation of Sc_2Te_3 (NaCl type with disordered cation vacancies). The elements (Sc, 99.7%, Aldrich-APL; Te powder, 99.99%, Alfa-AESAR) were loaded as received in 2:3 proportions into a fused silica tube. This was sealed under vacuum and heated to 450 °C for 12 h, and then to 900 °C for 72 h. Guinier film data confirmed the production of only the target phase. This and the appropriate amount of scandium metal and silver powder (99.7% Fisher) to give a 6:1:2 (Sc:Ag:Te) stoichiometry were then pelletized with the aid of a hydraulic press within a glovebox. The pellet was arc-melted within the glovebox for 20 s per side with a current of 40 A. A Guinier pattern of the product at this point revealed single-phase (>95%) orthorhombic Sc_6AgTe_2 . This was annealed at 1135 °C for 48 h inside a welded tantalum container¹⁶ with an intermediate Mo foil to lessen loss of Ag into the container, after which it was cooled at 1 °C/h to 800 °C and then allowed to cool radiatively. According to the powder diffraction data, the Sc_6AgTe_2 had been obtained in high yield, a small amount of ScTe (NiAs type) also being present (5–10%). Single crystals therein were selected for structural analysis. The compound Sc_6AgTe_2 appears to be stable in air for periods of weeks.

The analogous copper reaction was loaded with Sc metal, Cu powder (99.7%, Fisher), and Sc_2Te_3 in a Sc:Cu:Te ratio 6:1:2, reacted with similar procedures, and single crystals therefrom were selected for structural analysis. The product $Sc_6Cu_{0.80(2)}Te_{2.20(2)}$ according to the X-ray study (below) is similarly stable in air for a couple of weeks. Concerning a possible copper variability, two more reactions were run with Sc:Cu:Te proportions 6:1.2:2 and 6:1.5:2 and the same procedure and heating cycles. On the basis of Guinier powder data, the unit parameters from the $Sc_6Cu_{1.2}Te_2$ reaction product were $a = 19.860(5)$ Å, $b = 3.910(1)$ Å, $c = 10.632(2)$ Å with 21 lines refined, and those for the $Sc_6Cu_{1.5}Te_2$ sample were $a = 19.872(5)$ Å, $b = 3.908(1)$ Å, $c = 10.636(3)$ Å with 17 lines refined. These are quite similar and scarcely different from data from the first reaction Sc_6CuTe_2 , 19.853(5) Å, 3.914(1) Å, 10.688(2) Å, indicating a substantially fixed upper limit Cu content in the phase. ScTe was the only other phase seen. After all three reactions, some copper-colored metal was found on the interior walls of the tantalum containers.

Sc:Cu:Te in the ratio 6:1:2 was loaded as an extension. Because of the low melting point of Cd metal (321 °C), we used CdTe (ZnS type) as starting material instead of Cd metal. The element Cd (99.7% Fisher) and Te were loaded in 1:1 proportions into a fused silica tube. This was sealed under vacuum and heated to 450 °C for 12 h, and then to 1050 °C for 72 h. Guinier film data confirmed

Table 1. Single Crystal X-ray Data Collection and Structure Refinement Parameters for Sc_6MTe_2 (M = Ag, Cu)

formula	Sc_6AgTe_2	$Sc_6Cu_{0.80(2)}Te_{2.20(2)}$
fw	632.80	601.3
cryst syst, space group, Z	orthorhombic, $Pnma$, 4	orthorhombic, $Pnma$, 4
lattice params ^a (Å, Å ³)	$a = 20.094(9)$ $b = 3.913(1)$ $c = 10.688(2)$ $V = 840.4(5)$	$a = 19.853(5)$ $b = 3.914(1)$ $c = 10.644(2)$ $V = 827.1(3)$
d_{calc} (g/cm ³)	5.002	4.73
μ , mm ⁻¹ (Mo K α)	13.537	13.957
R1, wR2 ^b for $I > 2\sigma(I)$	0.024, 0.057	0.028, 0.062

^a Guinier data obtained with Cu K α radiation ($\lambda = 1.54050$ Å) at 23 °C with 15, 20 indexed lines, respectively. ^b $R1 = \sum ||F_o| - |F_c|| / \sum |F_o|$; $wR2 = \{ \sum [w(F_o^2 - F_c^2)^2] / \sum [w(F_o^2)^2] \}^{1/2}$. For Sc_6AgTe_2 : $w^{-1} = [\sigma^2(F_o^2) + (0.0327p)^2 + 1.3898p]$, where $p = (F_o^2 + 2F_c^2)/3$. For $Sc_6Cu_{0.80(2)}Te_{2.20(2)}$: $w^{-1} = [\sigma^2(F_o^2) + (0.0310p)^2]$, where $p = (F_o^2 + 2F_c^2)/3$.

a single-phase product of CdTe (>95% yield). This and an appropriate amount of Sc metal and Sc_2Te_3 powder to give a 6:1:2 (Sc:Cu:Te) stoichiometry were loaded within a He-filled glovebox with a procedure similar to that used in the synthesis of Sc_6AgTe_2 . The weight loss during arc-melting was around 10%. After annealing at 1135 °C for 48 h, the powder diffraction data showed that the sample contained ~80% Sc_6CdTe_2 and 20% ScTe (NiAs type). Black well-shaped single crystals were also found inside the Ta tube. A new phase Sc:Cu:Te = ~3:1:1 was also found.

Single-Crystal Diffraction. Several black, irregularly shaped crystals of Sc_6AgTe_2 were selected and sealed inside 0.3-mm i.d. thin-walled capillaries. Crystal qualities were checked with Laue photographs, and the best crystal was taken for a data set collection on a Bruker SMART 1000 CCD-based X-ray diffractometer at room temperature with Mo K α_1 radiation. A total of 1259 frames were collected with the exposure time of 45 s per frame. The reflection intensities were integrated with the SAINT subprogram in the SMART software package,¹⁸ and an absorption correction was applied with the aid of the package program SADABS.¹⁹ Of 3241 measured reflections, 1042 were unique and 975 had $I > 2\sigma(I)$. The structure was solved by direct methods and refined with the SHELXS¹⁷ package in the indicated space group $Pnma$. After isotropic refinement, the final anisotropic refinement converged at $R1, wR2 = 2.39/5.74\%$ for the composition Sc_6AgTe_2 . Some data for these processes are listed in Table 1, and the atomic positions and isotropic-equivalent temperature factors are given in Table 2.

The crystal qualities for the product of the synthesis reaction Sc_6CuTe_2 were checked with Laue photographs, and then the best crystal was transferred to a Bruker SMART 1000 CCD-based X-ray diffractometer for data collection at room temperature with Mo K α_1 radiation. A total of 1244 frames were collected with the exposure time of 60 s per frame. The reflection intensities were integrated with the SAINT subprogram in the SMART software package¹⁸ for the orthorhombic unit cell. This process yielded a total of 3149 reflections out of which 1120 were independent and 948 had intensities greater than $2\sigma(I)$. The XPREP subprogram in the SHELXTL software package¹⁷ was used for the space group determination, for which systematic absences again indicated $Pnma$. An absorption correction was applied with the package program SADABS.¹⁹ All the atomic positions were located by direct methods and successfully refined with the SHELXTL¹⁷ program. Some data collection and refinement parameters are given in Table 1. The complete positional and isotropic-equivalent thermal parameters for

(14) Maggard, P. A.; Corbett, J. D. *J. Am. Chem. Soc.* **2000**, *122*, 10740.

(15) Maggard, P. A.; Corbett, J. D. *Inorg. Chem.* **1999**, *38*, 1945.

(16) Corbett, J. D. *Inorg. Synth.* **1983**, *22*, 15.

(17) SHELXTL; Bruker AXS, Inc.: Madison, WI, 1997.

(18) SMART; Bruker AXS, Inc.: Madison, WI, 1996.

(19) Blessing, R. H. *Acta Crystallogr.* **1995**, *A51*, 33.

Table 2. Positional and Isotropic-Equivalent Thermal Parameters ($\text{\AA}^2 \times 10^3$) for Sc_6AgTe_2 and $\text{Sc}_6\text{Cu}_{0.80(2)}\text{Te}_{2.20(2)}$ ^a

atom	<i>x</i>	<i>z</i>	<i>U</i> _{eq} ^b
Sc₆AgTe₂			
Ag1	0.0742(1)	0.1419(1)	11(1)
Te2	0.3738(1)	0.2744(1)	11(1)
Te3	0.2636(1)	0.4667(1)	10(1)
Sc1	0.3926(1)	0.8345(1)	15(1)
Sc2	0.3388(1)	0.5351(1)	13(1)
Sc3	0.2286(1)	0.2494(1)	12(1)
Sc4	0.0306(1)	0.8782(1)	15(1)
Sc5	0.1385(1)	0.5679(1)	13(1)
Sc6	0.4910(1)	0.1081(1)	17(1)
Sc₆Cu_{0.80(2)}Te_{2.20(2)}			
Cu1 ^c	0.0743(1)	0.1414(1)	10(1)
Te2	0.3749(1)	0.2742(1)	10(1)
Te3	0.2627(1)	0.4662(1)	10(1)
Sc1	0.3926(1)	0.8302(2)	15(1)
Sc2	0.3428(1)	0.5365(1)	16(1)
Sc3	0.2281(1)	0.2496(1)	12(1)
Sc4	0.0271(1)	0.8792(2)	19(1)
Sc5	0.1379(1)	0.5671(1)	11(1)
Sc6	0.4929(1)	0.1089(1)	15(1)

^a All atoms on 4*c*, *m*; *y* = 1/4. ^b *U*_{eq} is defined as one-third of the trace of the orthogonalized *U*_{*ij*} tensor. ^c Occupancy of this site is 0.80(2) Cu, 0.20(2) Te.

what refined to be $\text{Sc}_6\text{Cu}_{0.80(2)}\text{Te}_{2.20(2)}$ are given in Table 2. The Cu1 site was occupied by 0.80(2) copper and 0.20(2) tellurium when these two atoms were fixed at the same site and with the same anisotropic parameters, the sum was constrained to 100% occupancy,¹⁷ and all other variables were free. This phenomenon of late-transition-metal and nonmetal occupancies on the same sites is known to happen in some ternary phases, as in $\text{Hf}_5\text{Co}_{1+x}\text{P}_{3-x}$.^{10d} Additional data collection, refinement, atom positional and anisotropic displacement parameters, and all interatomic distances for both structures are given in the Supporting Information. These as well as the *F*_o/*F*_c listings are available from J.D.C.

Band Calculations. All the extended Hückel band calculations were carried out using the CAESAR program.²⁰ The valence-state ionization energies (*H*_{*ii*}'s) of Sc and Te were taken from the values iterated to charge consistency for Sc_2Te .⁷ The *H*_{*ii*}'s of Pd, Ag, Cu were obtained from charge iterative calculations²¹ on the respective Sc_6MTe_2 (M = Pd, Ag, Cu). The atom parameters used are listed in Table 3.

Results and Discussion

Structural Description. The new Sc_6CuTe_2 and Sc_6AgTe_2 are isostructural with Sc_6PdTe_2 ,¹⁴ and here we describe just the structure of Sc_6AgTe_2 in detail. A near-[010] section of the Sc_6AgTe_2 structure viewed along the short *b* axis is given in Figure 1 with Sc as blue (Sc1–3, Sc5, Sc6) or black (Sc4), Te as red, and Ag as yellow spheres. The structure can be described as the result of a polymerization of two kinds of scandium metal chains, which were formerly described in Sc_2Te ⁷ as separate double octahedral chains or blades (blue) and zigzag chains (black), via displacement of the Te1 atom by a strongly bonding heterometal Ag, etc. The resulting condensed heterometal sheets in the product are still separated by isolated tellurium atoms (red) along the *a* axis. The

Table 3. Extended Hückel Parameters

atoms	orbital	<i>H</i> _{<i>ii</i>} (eV)	ζ_1	<i>c</i> ₁	ζ_2	<i>c</i> ₂
Sc	4s	−6.74	1.30			
	4p	−3.38	1.30			
	3d	−6.12	4.35	0.4228	1.700	0.7276
Te	5s	−21.20	2.51			
	5p	−12.00	2.16			
Ag ^a	5s	−7.00	2.24			
	5p	−3.28	2.24			
	4d	−12.39	6.07	0.5889	2.663	0.6370
Cu ^a	4s	−6.99	2.20			
	4p	−3.44	2.20			
	3d	−10.66	5.95	0.5933	2.300	0.5744
Pd ^a	5s	−5.04	2.19			
	5p	−1.94	2.15			
	4d	−8.76	5.98	0.5535	2.613	0.6701

^a The starting values for charge iteration of Ag, Cu, and Pd came from Alvarez (S. Alvarez, Tables of Parameters for Extended Hückel Calculations, Parts 1 and 2, Barcelona, Spain, 1993), namely, Ag (metal) 5s, −7.56, 2.244; 5p, −3.83, 2.244; 4d, −11.58, 6.07 (0.5889), 2.663 (0.6370); Cu 4s, −11.4, 2.2; 4p, −6.06, 2.2; 3d, −14.0, 5.95 (0.5933), 2.30 (0.5744); Pd 5s, −7.32, 2.19; 5p, −3.75, 2.152; 4d, −12.02, 5.983 (0.5535), 2.613 (0.6701).

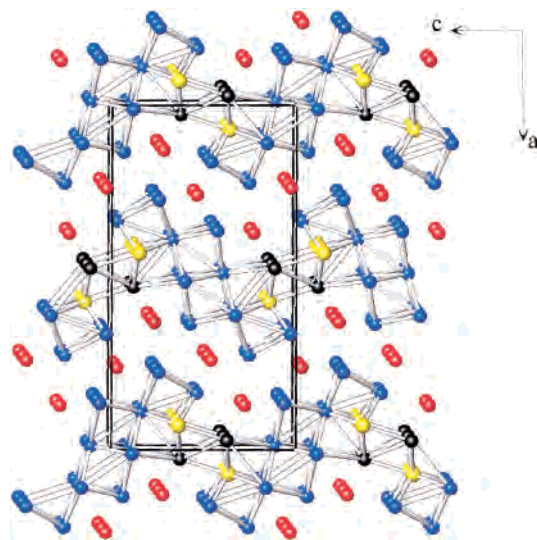


Figure 1. An $\sim[010]$ view of the unit cell of Sc_6AgTe_2 . The blue atoms are scandium in the blade unit, the dark atoms are Sc4 that form the zigzag chains, the yellow atoms are silver, and red atoms are tellurium. The structure is infinite along the view direction.

compound was synthesized directly in high yield, but should one describe this in terms of the structural conversion, the net disproportionation reaction is



Some important bond distances are given in Table 4. There are no short Te–Te separations so their problematic bonding is not a concern. The metal environments of Te2 and Ag are monocapped trigonal prisms whereas that of Te3 is a bicapped example. Sc–Te distances range between 2.87 and 3.12 Å, less than nearly all Sc–Sc distances.

Figure 2 illustrates a portion of a single heterometal sheet down the *b* axis plus the atom labels and distances with a similar but lighter color scheme relative to Figure 1. (There is an inversion center on the short Sc6–Sc6 bond.) The important metal–metal distances and their respective overlap populations are given in Table 4. The condensed double octahedral chain (Sc blade) composed of Sc1, Sc5, Sc6, Sc2,

(20) Ren, J.; Liang, W.; Whangbo, M.-H. *CAESAR for Windows*; Prime-Color Software, Inc., North Carolina State University: Raleigh, NC, 1998.

(21) Whangbo, M. H.; Li, J. *CIBAND*; Dept. of Chemistry, North Carolina State University: Raleigh, NC, 1995.

Table 4. Selected Bond Distances (Å) and Mulliken Overlap Populations (MOP)

contact	Sc_2Te		Sc_6AgTe_2		$Sc_6Cu_{1.0}Te_2$		Sc_6PdTe_2	
	bond	MOP	bond	MOP	bond	MOP	bond	MOP
Sc6–Sc6	3.05	0.366	3.05	0.340	3.04	0.327	3.08	0.322
Sc1–Sc6	3.13	0.288	3.11	0.283	3.07	0.304	3.11	0.299
Sc1–Sc5	3.20	0.172	3.23	0.156	3.24	0.146	3.32	0.129
Sc5–Sc6 ^a	3.52	0.170	3.50	0.175	3.44	0.193	3.40	0.220
Sc1–Sc6 ^a	3.49	0.166	3.53	0.124	3.57	0.110	3.86	0.057
Sc5–Sc6	3.27	0.146	3.28	0.122	3.28	0.117	3.34	0.107
Sc1–Sc3	3.25	0.119	3.25	0.161	3.21	0.176	3.23	0.174
Sc2–Sc3	3.32	0.087	3.31	0.127	3.31	0.124	3.30	0.138
Sc1–Sc2	3.42	0.069	3.38	0.173	3.28	0.207	3.20	0.250
Sc4–Sc6	3.53	0.035	3.51	0.060	3.50	0.060	3.49	0.071
Sc4–Sc4	3.48	0.026	3.48	0.122	3.40	0.070	3.39	0.171
Sc1–Sc4	3.67	0.025	3.59	0.108	3.48	0.134	3.42	0.167
M–Sc1 ^b	2.95	0.234	2.92	0.149	2.88	0.122	2.78	0.122
M–Sc2	2.90	0.274	2.86	0.169	2.79	0.160	2.79	0.134
M–Sc4	2.90	0.273	2.88	0.164	2.82	0.147	2.83	0.121
M–Sc4	2.93	0.267	2.95	0.166	2.94	0.130	2.91	0.118

^a Across octahedra; the latter is marked in Figure 1. ^b M = Te1 in Sc_2Te .

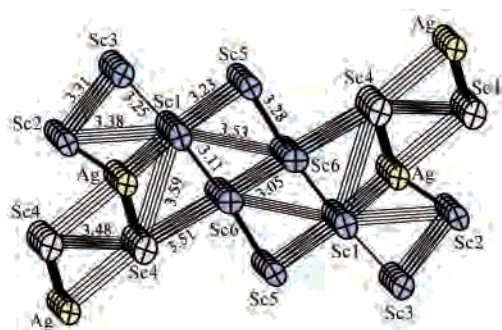


Figure 2. Details of the highly condensed double octahedra chains or blades (blue Sc1, Sc5, Sc6, Sc2, Sc3) and zigzag chains (gray Sc4–Sc4) that are bonded together via silver atoms (yellow) to form infinite sheets (98% probability thermal ellipsoids).

Sc3 and formerly isolated zigzag chain Sc4–Sc4 are now adjoined through bonding with Ag. Compared with Sc_2Te ,⁷ the zigzag chain has moved toward the double chain, with $d(Sc4–Sc1)$ decreasing from 3.67 to 3.58 Å and $d(Sc4–Sc6)$, from 3.53 to 3.51 Å, whereas $d(Sc4–Sc2)$ keeps the same 3.68 Å separation. For comparison, these values in Sc_6CuTe_2 and Sc_6PdTe_2 are a little less: 3.48, 3.42; 3.50, 3.49; and 3.65, 3.66 Å, respectively. The bonds within the imagined octahedra (Sc5–Sc6 height, and Sc1–Sc6 waist, marked) are 3.52, 3.49 Å in Sc_2Te , 3.50, 3.53 Å in Sc_6AgTe_2 , 3.44, 3.57 Å in Sc_6CuTe_2 , and 3.40, 3.86 Å in Sc_6PdTe_2 , respectively; that is, shortest for Cu and Pd in the former. From this point of view, one gains a sense that these condensed double octahedra can be distorted quite a lot, which may be one of the reasons that this orthorhombic structure is stable with different metals. Of course, the stability range also depends on the stability of alternate phases, which is seldom known.

A great many metal-rich phases share one common feature, a short repeat axis that appears to be determined primarily by the van der Waals radii of the anions.²² These three Sc_6MTe_2 phases have nearly the same *b* axis, ~3.91 Å. The M–Sc distances vary over 2.86–2.96 Å in Sc_6AgTe_2 ,

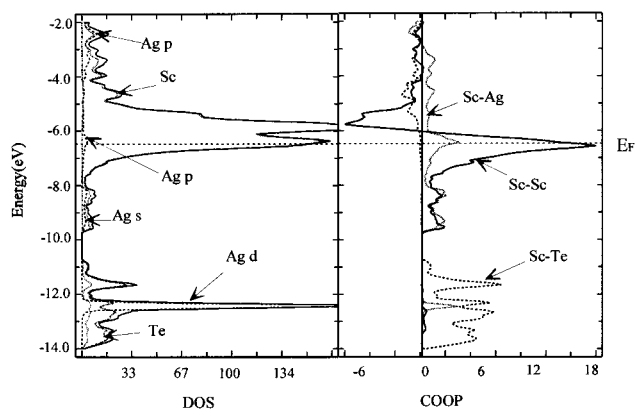


Figure 3. DOS and COOP plots calculated for Sc_6AgTe_2 . In DOS, the solid, dotted, dashed, and dash-dotted lines refer to total DOS and partial DOS of Sc, Ag, and Te, respectively. In the COOP plots, the solid, dotted, and dashed lines represent data for all Sc–Sc bonds within 3.6 Å, all Sc–Ag contacts within 3.0 Å, and all Sc–Te interactions within 3.0 Å, respectively.

2.79–2.94 Å in $Sc_6Cu_{0.8}Te_{2.2}$, and 2.78–2.91 Å in Sc_6PdTe_2 . Internal Sc–Sc distance trends remain similar to those in Sc_2Te .⁷ Naturally the observed Sc–Cu distances reported include the effect of an ~20% Te population on that site.

Theoretical Calculations. Extended Hückel tight-binding band calculations for all three Sc_6MTe_2 give quite similar band structures. Here we describe only those for Sc_6AgTe_2 as an example. Figure 3 shows the total and some partial DOS plus Sc–Sc, Sc–Ag, and Sc–Te COOP data for Sc_6AgTe_2 . (Of course, 100% Cu on the bridging site has necessarily been assumed.) As is usual for such compounds, the Fermi level is located on the low-energy side of a large band that is generated mostly by Sc 3d orbitals, with a small Ag 5p contribution around E_F . Scandium 4s and silver 5s states comprise essentially all of the lower valence bands between ~−9.5 and −8.0 eV, with silver 4d states being the majority at ~−12.4 eV in a peak that is surrounded by those originating from Te 6p at −11 to −14 eV. There is only one appreciable difference among the results for the three Sc_6MTe_2 compounds, namely, that the large and narrow d^{10} band of M varies from ~−12.2 to −12.7 eV for Ag 4d to ~−8.5 to −9.0 eV for Pd 4d, with Cu 3d being intermediate. Other features of the electron structures of these compounds remain nearly the same. Regarding the valence electron concentrations, even though Cd, Ag, and Cu have two, one, and one electron differences from Pd, the Sc metal network appears to serve as an electron reservoir for additional electrons and Sc–Sc bonding. This is primarily because of the large number of Sc–Sc bonding states present at and above the Fermi level.

Figure 3 also shows the crystal orbital overlap population (COOP) curves for Sc–Sc, Sc–Ag, and Sc–Te bonding. The COOP curves show that both Sc–Sc and smaller Sc–Ag contributions are highly bonding up to and beyond E_F . This is typical for these electron-deficient metallic compounds.^{7,14,15}

The strength of the pairwise bonding interactions can be qualitatively related in terms of COOP data (Figure 3, right) and the corresponding Mulliken overlap populations (MOP).

(22) Maggard, P. A.; Corbett, J. D. *J. Am. Chem. Soc.* **2000**, *122*, 838.

Table 5. Effective Atom Charges in Sc_6MTe_2 ($\text{M} = \text{Ag}, \text{Cu}, \text{Pd}$) (Mulliken Approximation)

Sc_6AgTe_2		Sc_6CuTe_2		Sc_6PdTe_2		Sc_2Te	
atom	charge	atom	charge	atom	charge	atom	charge
Sc1	-0.79	Sc1	-0.90	Sc1	-0.79	Sc1	-0.56
Sc2	0.94	Sc2	0.93	Sc2	0.90	Sc2	1.17
Sc3	0.69	Sc3	0.70	Sc3	0.69	Sc3	0.72
Sc4	0.96	Sc4	0.91	Sc4	0.85	Sc4	1.31
Sc5	0.61	Sc5	0.71	Sc5	0.75	Sc5	0.44
Sc6	-1.03	Sc6	-0.97	Sc6	-0.91	Sc6	-1.20
Ag	-0.08	Cu	-0.03	Pd	-0.18	Te1	-0.55
Te2	-0.65	Te2	-0.67	Te2	-0.67	Te2	-0.67
Te3	-0.65	Te3	-0.68	Te3	-0.66	Te3	-0.65

The MOP values for neighboring pairs of atoms in Sc_2Te and Sc_6MTe_2 ($\text{M} = \text{Ag}, \text{Cu}, \text{Pd}$) are listed in Table 4. (Notice how poorly certain of these scale with distance.) In the parent Sc_2Te , the largest Sc–Sc MOP values are Sc6–Sc6 (MOP 0.366) and Sc1–Sc6 (0.288) on the interior of the double octahedra (Figure 2). All the Sc–Sc MOP for the central part of the former blade range between 0.146 and 0.366. On the other hand, the MOP are lower, 0.069–0.11, within the Sc1, Sc2, Sc3 appendages and only 0.026 within the zigzag chains Sc4–Sc4. The bonding of Sc4 to all other scandium atoms is relatively weak (<0.035). However, after insertion of the silver atoms, which bridge between the two substructures, both the zigzag chains Sc4–Sc4 and appendage chains (Sc1, Sc2, Sc3) show larger MOP values and shorter interatomic distances. For example, the Sc4–Sc4 MOP increases from 0.026 to 0.122, and Sc1–Sc2 from 0.069 to 0.173. The apparently strongest bonding interactions still remain within Sc6–Sc6 (0.340) and Sc1–Sc6 (0.283). The relative heteroatomic Sc–Te, Sc–Cu, and Sc–Ag bonding would be assigned somewhat higher “strengths” were the better approximations given by Hamiltonian populations to be considered.²³

The DOS data for Ag in Figure 3 are particularly remarkable in the large dispersion of the Ag 4d, 5s, and 5p contributions. The narrow 4d band near -12.5 eV matches only a small Sc–Ag contribution in the COOP. The small and broader band between about -8.0 and -10.0 eV originates mainly from Sc 3s–Ag 5s and Sc 3s–Sc 3s interactions. The Sc 4p states make small contributions only at E_F and above -4.0 eV. (Copper shows similar effects.)

Table 5 lists the effective atom charges in Sc_6MTe_2 ($\text{M} = \text{Ag}, \text{Cu}, \text{Pd}$) and Sc_2Te according to the Mulliken approximation (in which bonding electrons in heteroatomic pair interactions are split equally). Of course, these can be given only semiquantitative meanings at most, but they seem to be the best way to summarize the relative effects of the variety of distances and neighbors about each atom. Naturally, all tellurium atoms have a negative charge (≤ -0.55). And because of the covalent bonding interactions between Te and nearest neighbor Sc, the Sc 3d states on the surface of the sheets are “pushed up”, and the surface atoms (Sc2, Sc3, Sc4, Sc5) of the sheet (see Figure 2) acquire a relatively positive charge (0.44–1.31 in Sc_2Te), whereas all the inner atoms (Ag, Cu, Pd, Sc1, Sc6) have relative negative charges

(-0.56 to -1.20 in Sc_2Te , -0.03 for Cu to -0.18 for Pd). This parallels and helps explain the Mulliken overlap populations in Table 4 in which the two largest values occur between the interior Sc6–Sc6 and Sc1–Sc6 and, compared with other scandium atoms types, both Sc1 and Sc6 have large PDOS peaks around and below E_F (not shown). In other words, there is an electron flow from surface Sc2, Sc3, Sc4, Sc5 both to nonmetal Te atoms and to inner atoms (Sc1, Sc6 and Ag/Cu/Pd). Accordingly, overlap populations between surface Sc atoms are also substantially smaller, as been noted in other Sc–Te phases as well.^{5,22} The charge distribution shows a similar but somewhat greater trend in Sc_2Te , because Te1 atom removed has a larger electronegativity (lower H_{ii}) than Ag, Cu, or Pd, and so all of the scandium atoms about Te1, namely, Sc1, Sc2, and Sc4, have more positive values compared with those in the ternary compounds.

In summary, on the basis of the extended Hückel calculations, it can be said that, in Sc_6MTe_2 , the metal–metal bonding interactions spread throughout the newly formed metal sheets (as shown in Figure 2), whereas in Sc_2Te , the metal–metal interactions are concentrated on the core unit, leaving two metal chains separated by tellurium atoms. And we gain the impression that the broad band of bonding states in the metal network in this orthorhombic structure can both serve as an empty reservoir for electrons and give additional M–M bonding. Thus the electron count of M is not of overwhelming importance, and even some electron-rich elements such as In, Bi, etc. may possibly be introduced in this type of structure. A rich and novel chemistry seems possible.

Conclusion

The structures of Sc_6MTe_2 ($\text{M} = \text{Ag}, \text{Cu}, \text{Pd}$) can be viewed as packed heterometal sheets parallel to the b – c planes that are separated by layers of isolated tellurium atoms along the a axis. The sheet is achieved via polymerization of two types of scandium chains through substitution of tellurium spacers with later transition metals Ag, Cu, or Pd. Extended Hückel calculations show that the introduction of heterometal bonding in place of that of Te enhances the approximate bond strengths to neighboring Sc atoms in the formation of the condensed heterometal sheet (Figure 2). The new calculational data illustrate how the Sc metal atoms are differentiated according to how many Te neighbors they have, the greater nonmetal interactions in effect oxidizing the Sc neighbors and diminishing their Sc–Sc bonding.

Acknowledgment. Evidence for the copper compound was first acquired by Paul Maggard. This research was supported by the National Science Foundation, Solid State Chemistry, via Grant DMR-9809850 and was carried out in the facilities of the Ames Laboratory, U.S. Department of Energy.

Supporting Information Available: More information on X-ray data collection and refinement plus anisotropic displacement parameters and listings of all bond lengths for/in Sc_6AgTe_2 and $\text{Sc}_6\text{Cu}_{0.80}\text{Te}_{2.2}$. This material is available free of charge via the Internet at <http://pubs.acs.org>.

(23) Glassey, W. V.; Hoffmann, R. *J. Chem. Phys.* **2000**, *113*, 1698.